Time-dependent wind on Advection-Diffusion-Reaction system

Computational Physics project

Giuseppe Sacco

September 2021

1 Introduction

The combined effect of advection, diffusion and reaction on a single-species population can give rise to very interesting behaviour, especially when heterogeneities are introduced.

In this paper we study the effect of a wind variable in time and constant in space on a 2D system. Results will be systematically compared to its constant-wind counterpart in order to highlight those features that are due to the variability of the wind.

2 Presentation of the system

The time evolution of the general Advection-Diffusion-Reaction system can be described by the equation

$$\frac{\partial c(\mathbf{x},t)}{\partial t} = -\nabla \cdot [\mathbf{U}(\mathbf{x},t)c(\mathbf{x},t)] + \nabla \cdot [D(\mathbf{x},t)\nabla c(\mathbf{x},t)] + R(c,\mathbf{x},t) \qquad (1)$$

where c is the density of the population transported by the wind of velocity $\mathbf{U}(\mathbf{x},t)$. Diffusion is governed by the coefficient $D(\mathbf{x},t)$ and local chemistry is represented by $R(c,\mathbf{x},t)$.

In this work, we will make the following assumptions:

- $\mathbf{U}(\mathbf{x},t) = (U_x(t), 0)$
- $D(\mathbf{x},t) = D$
- $R(c,\mathbf{x},t) = R(c,\mathbf{x}) = a(\mathbf{x})c(\mathbf{x},t) - bc^2(\mathbf{x},t)$

where a is the Mathus growth rate and b is the competition coefficient.

Eq.1 can than be rewritten as

$$\frac{\partial c(\mathbf{x},t)}{\partial t} = -U_x(t)\frac{\partial}{\partial x}c(\mathbf{x},t) + D\nabla^2 c(\mathbf{x},t) + R(c,\mathbf{x}) \qquad (2)$$

2.1 Discretization

Upon discretization of the space-time (2+1D), eq.2 can be expressed through the ADR transfer matrix formalism:

$$\frac{c_{ij}^{n_t+1} - c_{ij}^{n_t}}{h} = \left[\frac{U^{n_t}}{d} A_{ijkl} + \frac{D}{d^2} D_{ijkl} + R\delta_{ij,kl}\right] c_{kl}^{n_t} \tag{3}$$

with

$$n_t = 1, ..., N_t \qquad i, k = 1, ..., N_y \qquad j, l = 1, ..., N_x$$

where d and h are the lenght of the space and time steps and forward Euler for time evolution has been used. A, D, R are the discrete version of the operators of Eq.2.

Since we are considering the wind blowing only in the x direction (first assumption), than A_{ijkl} will be non zero only for $A_{i,j,i,j+1} = 0.5$ and $A_{i,j,i,j-1} = -0.5$ (corresponding to the centered-forward discretization of $\frac{\partial}{\partial x}$). For the diffusion operator the laplacian has been discretised to a nine-point stencil where non-zero elements are $D_{ijij} = -3$ (center), $D_{i,j,i+1,j} = D_{i,j,i,j+1} = D_{i,j,i-1,j} = D_{i,j,i,j-1} = 0.5$ (sides), $D_{i,j,i+1,j+1} = D_{i,j,i-1,j+1} = D_{i,j,i-1,j-1} = D_{i,j,i+1,j-1} = 0.25$ (corners), as represented below.

$$\begin{array}{r} \\ i-1 \\ i \\ i+1 \end{array} \begin{array}{c} \begin{array}{ccc} j-1 & j & j+1 \end{array} \\ \begin{pmatrix} 0.25 & 0.5 & 0.25 \\ 0.5 & -3 & 0.5 \\ 0.25 & 0.5 & 0.25 \end{pmatrix} \end{array}$$

Since the reaction operator acts locally, $\delta_{ij,kl}$ corresponds to the Dirac delta (non-zero only when $i = k$, $j = l$).

By multiplying both sides for h, Eq.3 can be rewritten as

$$c_{ij}^{n_t+1} - c_{ij}^{n_t} = \left[\alpha^{n_t} A_{ijkl} + \delta D_{ijkl} + \rho\delta_{ij,kl}\right] c_{kl}^{n_t} \tag{4}$$

where we have introduced the Courant-Friedrich-Levy coefficients

$$\alpha^{n_t} \equiv \frac{U^{n_t} h}{d} \qquad \delta \equiv \frac{Dh}{d^2} \qquad \rho \equiv Rh$$

For the chemical time marching the exact nonlinear propagator is applied

$$R_{prop} = \frac{e^{ah}}{1 + c(e^{ah} - 1)\frac{a}{b}}$$

In order to solve the full ADR, SWSS operator splitting is used:

$$c^{n_t+1} = \frac{1}{2}[AD_{prop} R_{prop} + R_{prop} AD_{prop}] c^{n_t} \tag{5}$$

where $AD_{prop} = 1 + \alpha A + \delta D$ is the Advection-Diffusion propagator.

2.2 Parameters

For the purposes of this study, the space has been dicretised in a 128x128 uniform grid where periodic boundary conditions are applied.

For each site of the grid, the initial value of the population c_{ij}^0 is randomly sorted from the uniform distribution of the interval $[c_m - \delta_{c_m}, c_m + \delta_{c_m}]$ with $c_m = 1$, $\delta_{c_m} = 0.3$. Similarly, the Mathus growth rate for each site was sorted from $[a_m - \delta_a, a_m + \delta_a]$ with $a_m = 1$, $\delta_a = 2$, in such a way that while the overall ambient is fertile on average ($a_m > 0$), it is composed of oasis and deserts (since $\delta_a > a_m$). The diffusion CFL coefficient δ is set to 0.2. In order to shorten the transient behaviour of the system, it is useful to set $b = 1$ so that the average local capacity (a/b) equals c_m.[1]

All parameters are constant in time, the only exception being the wind (governed by the parameter α) that is varied sinusoidally with angular frequency $\tilde{\omega}$ according to the following equation

$$\alpha(t) = \alpha_0 + \delta_\alpha sin(\tilde{\omega} t) = \alpha_0 + \delta_\alpha sin(\omega n_t) \tag{6}$$

where in the last equality we have defined the adimensional $\omega \equiv \tilde{\omega} h$ and used $n_t = t/h$.

We will begin by briefly introducing the no-wind and constant wind case (respectively $\alpha(t) = 0$ and $\alpha(t) = 0.15$) and then compare it to the sinusoidal wind with $\alpha_0 = \delta_\alpha = 0.15$, $\omega = \frac{2\pi}{200}$ (the period will correspond to $n_t = 200$). Finally, in Sect 3.3 we see how the features studied for this particular case depend on each wind parameter[2] and draw some general trends.

3 Simulation

In Fig.1 we present the system in its initial condition as the population is randomly drawn at $n_t = 0$.

[1] Note that, because of the nonlinearity of the system, this does not imply that the average population will not change when introducing wind and diffusion.

[2] Effects of the phase of the sine in Eq.6 are neglected here since they involve only transient behaviour of the system, while we are interested on its stationary features.

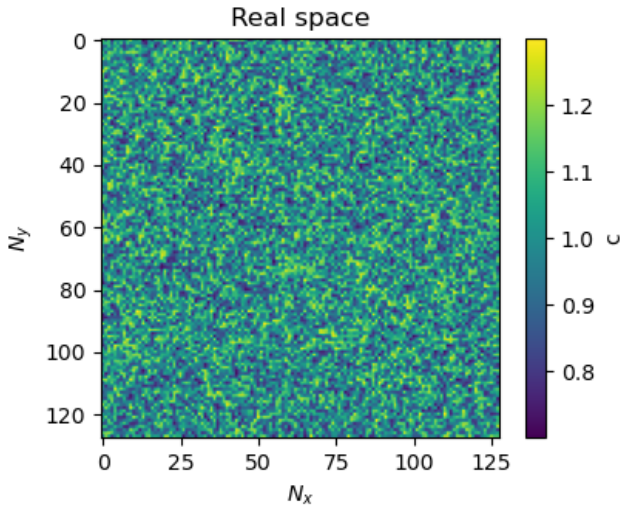

Figure 1: Initial condition of the randomly sorted population is represented as a colormap in the real space grid.

3.1 No-wind and constant wind case

The situation presented in Fig.1 evolves through a transient phase, after which both the no-wind case and constant wind system reach a stationary state, as represented in Fig.2. In order to better understand the properties of the system, we will also follow the evolution of the amplitude of the population's Fourier Transform $|FT[c]|$, reported below the corresponding real space graphs. Notice how the wind breaks the system isotropy and forms stripes in the real space along the x axis. Correspondingly the amplitude of the Fourier transform is peaked in the origin and tightens along the k_x axis.

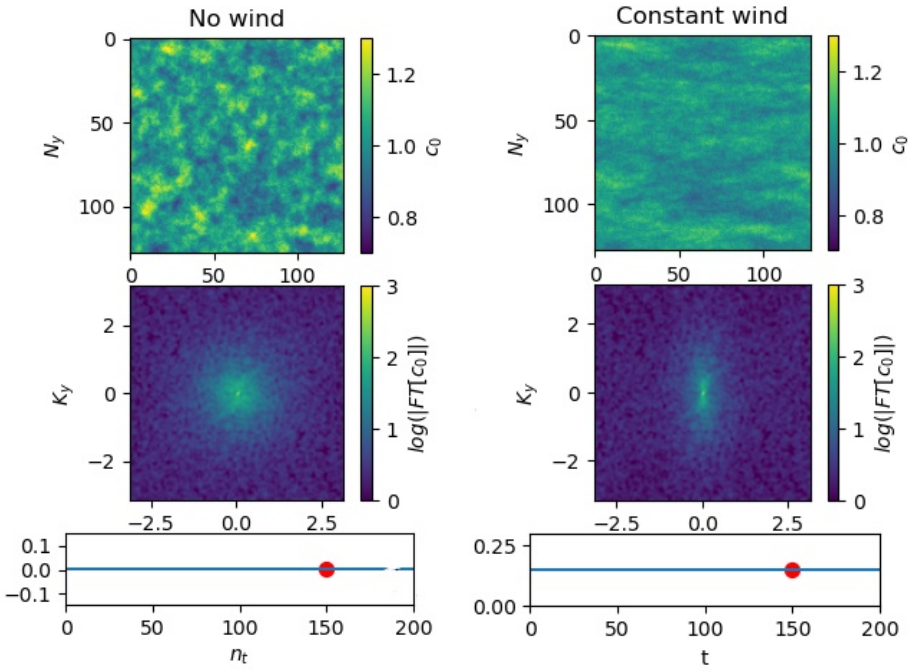

(a) $\alpha(t) = 0$. When advection is absent, the effects of local chemistry and diffusion are evident through the formation of diffused spots in the colormap. The corresponding FT amplitude is peaked in the origin and isotropicly shaped.

(b) $\alpha(t) = 0.15$. Stationary state corresponds to a striated pattern along the wind direction. Correspondingly, the Fourier transform amplitude is similar to the no-wind case but here isotropy is broken by the wind, tightening the peak along k_x.

Figure 2: Stationary state for the system when subjected to no wind (left) and a constant wind with $\alpha_0 = 0.15$ (right). Bottom plots represent the profile of $\alpha(t)$. Notice how fluctuation from the average population are mitigated by the wind. The Fourier transform amplitude is represented below each graph in logarithmic scale.

3.2 Sinusoidal wind

With the said choice of wind parameters, we can individuate three stages in the evolution of the system:

0. First period: mainly transient behaviour;
1. First half of each successive period: $|FT[c]|$ shows a rich pattern where relative minima and maxima are appearing and evolving;
2. Second half of each successive period: $|FT[c]|$ assumes a more isotropic shape due to the low values of the wind.

In Fig.3 we report the plots analogous to the previouses after one period, at the beginning of phase 1. To the colormaps referring to the sinusoidal wind (left column) we have added its constant wind counterpart (central column) that has already reached a stationary state, so it will be omitted hereafter. We will indicate with c_0 the population subjected to the constant wind, as opposed to c for the sinusoidal wind.

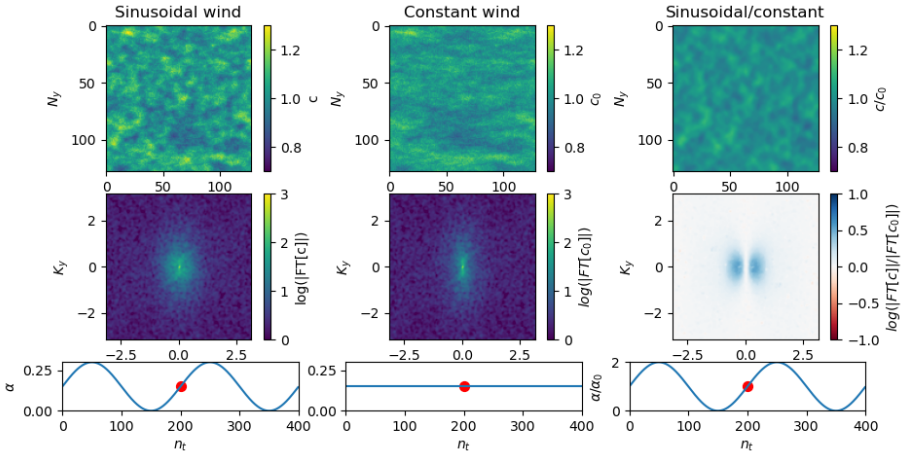

Figure 3: The plots are analogous to those of Fig.2, with the introduction of the sinusoidal wind (left column), here depicted after one period ($n_t = 200$). In the rightmost column a direct comparison in made by taking the ratios c/c_0 and $|FT[c]|/|FT[c_0]|$ (the latter in logarithmic scale). The FT amplitude of the sinusoidal wind system shows similar features to the constant wind counterpart. Notice however how it is more isotropic even though the values of α are exactly the same.

The sinusoidal wind counterpart shows similar features although it appears more isotropic. In the rightmost column the plots of c/c_0 and $|FT[c]|/|FT[c_0]|$ are shown in order to highlight the differences due to the wind variability. Notice how, right after the beginning of the period ($n_t = 205$, Fig.4), a second lobe of negative sign is appearing (light red in the figure).

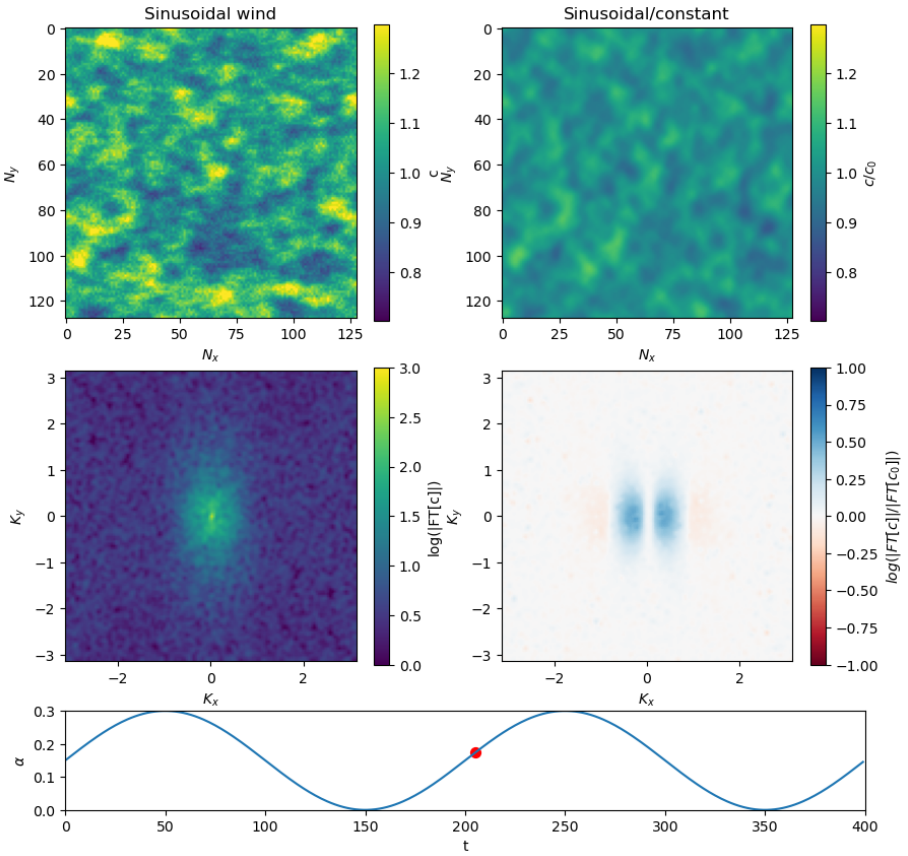

Figure 4: System at $n_t = 205$ (right after the beginning of the second period). Minima are beginning to appear in the plot of $|FT[c]|/|FT[c_0]|$. Plots referring to the constant wind are omitted because they reached their stationary state (they are shown in the central columns of Fig.3).

These minima appear centered in k_y (as shown above) and than separate in two lobes that migrate in opposite directions along k_y and move towards $k_x = 0$ while other relative maxima and minima are formed subsequently, as depicted in Fig.5 for $n_t = 235$.

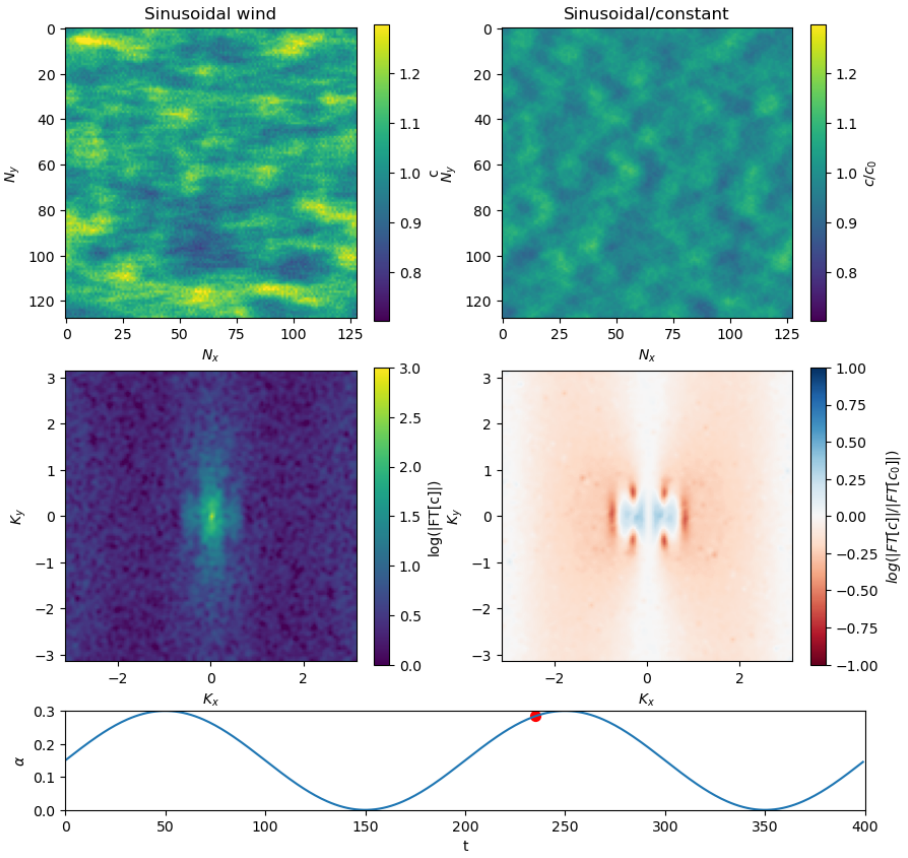

Figure 5: System at $n_t = 235$. Formation and migration of relative minima and maxima along the k_x, k_y plane due to variability of the wind are highlighted in the $|FT[c]|/|FT[c_0]|$ plot.

This pattern persists (see as an example Fig.6 for $n_t = 270$) until about $n_t = 300$, incidentally when $\alpha(t) = \alpha_0$ after half period.

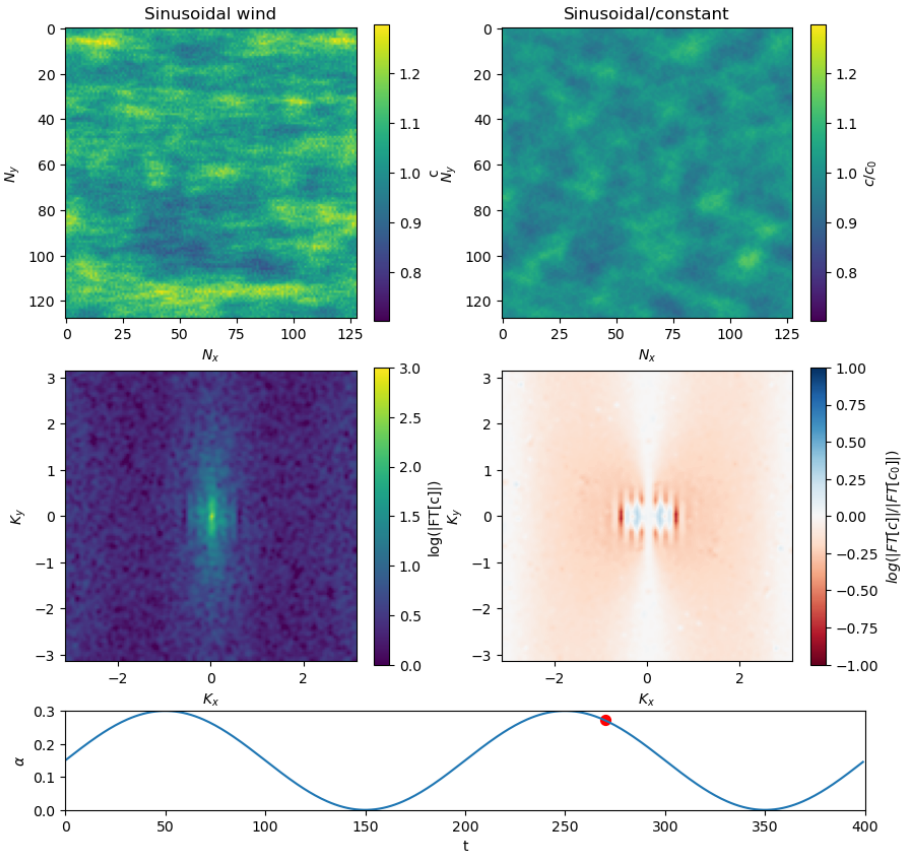

Figure 6: System at $n_t = 270$. The plot of $|FT[c]|/|FT[c_0]|$ shows the persistence and development of the trend described in the previous figures.

As anticipated, during the second half of the second period ($200 < n_t < 300$) the pattern described in Figs.3,4,5,6 vanishes and $|FT[c]|$ assumes a more isotropic shape because of the low value of $\alpha(t)$ in this region, as depicted in Fig.7.

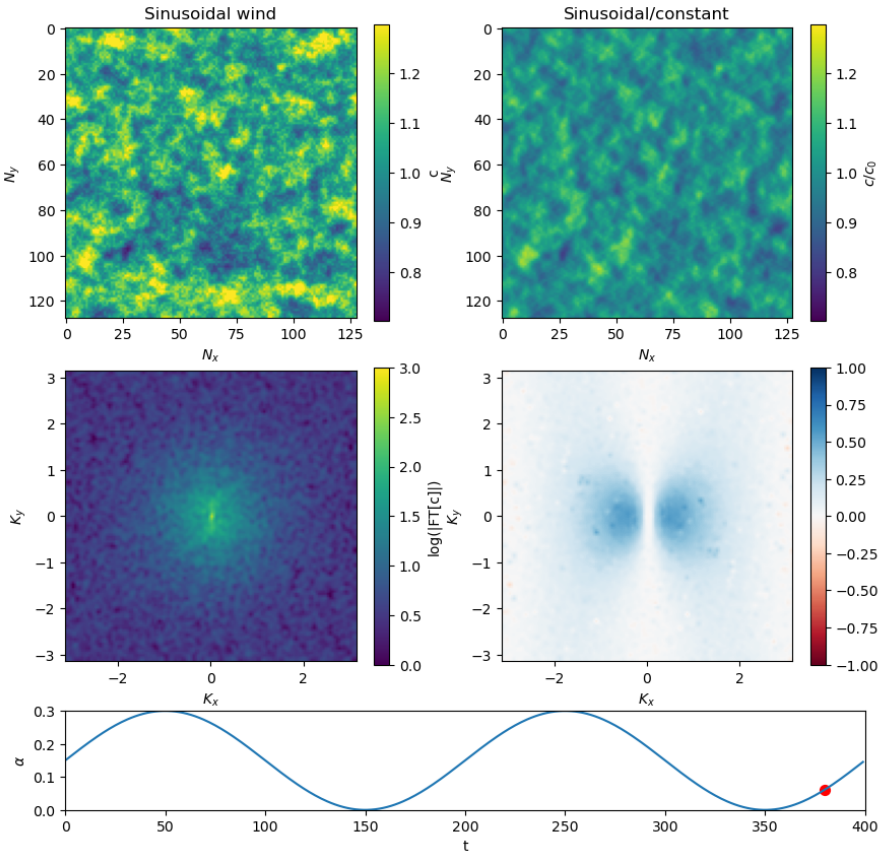

Figure 7: System at $n_t = 380$. $|FT[c]|$ assumes a more isotropic shape due to the low value of α; this results in the appearance of the blue lobes in the $|FT[c]|/|FT[c_0]|$ plot.

The behaviour described above is then repeated periodically with $\alpha(t)$.

The time evolution of the features observed in the previouses figures is summarised in Fig.8 where the colorbars represent the value of $|FT[c]|$, $|FT[c_0]|$, $|FT[c]|/|FT[c_0]|$ in the k_x, t plane at fixed k_y. In particular, the following figures are plotted for $k_y = 0$ and $k_y = \pi/4$.[3]

[3]The choice of $k_y = \pi/4$ is completely arbitrary, it is chosen as a value reasonably far from the origin in order to underline the differences with the plot for $k_y = 0$, but still close enough to the origin since this is the most interesting zone of the k_x, k_y plane.

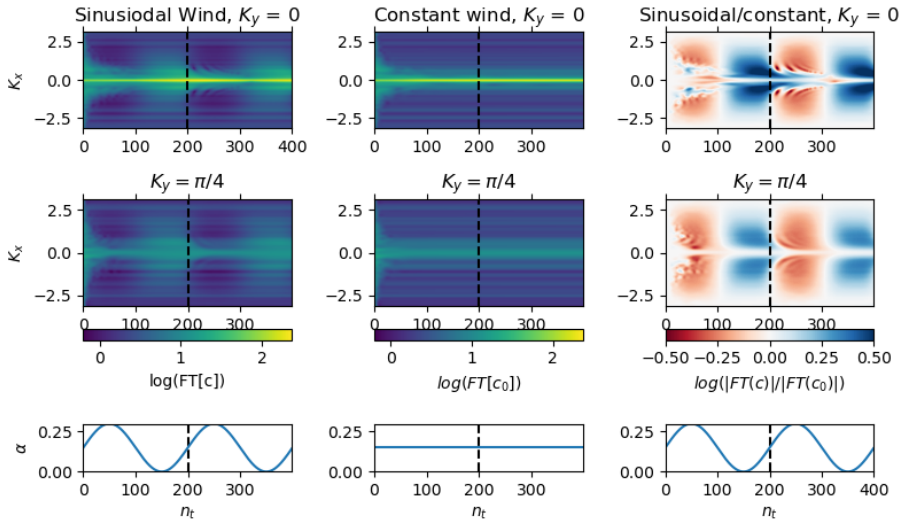

Figure 8: The colorbars represent, respectively from left to right, the value of $|FT[c]|$, $|FT[c_0]|$, $|FT[c]|/|FT[c_0]|$ (logarithmic scale) in the k_x, t plane at $k_y = 0$ (first row), $k_y = \pi/4$ (central row). Plots below show the wind profile; the dotted lines separate the periods. We retrieve the behaviour exposed above: transient phenomena dominate the first period, although we can already notice similarities with the stationary behaviour; during the first half of the subsequent periods we observe the creation and migration of relative minima/maxima; finally, the blue zones in the second half of the periods are due to the more isotropic shape of $|FT[c]|$, as discussed in the caption of Fig.6.

3.3 Dependence on wind parameters

So far we have considered the dynamics for $\alpha_0 = 0.15$, $\delta_\alpha = 0.15$, $\omega = \frac{2\pi}{200}$. An interesting comparison can be done setting $\alpha_0 = 0$ and leaving the others parameters unmodified. The results are presented in Fig.9 where we notice a pattern that resembles the one described in Fig.8 but with some interesting differences, notice for example how the periodicity is halved since the ratio $|FT[c]|/|FT[c_0]|$ does not depend the sign of α.

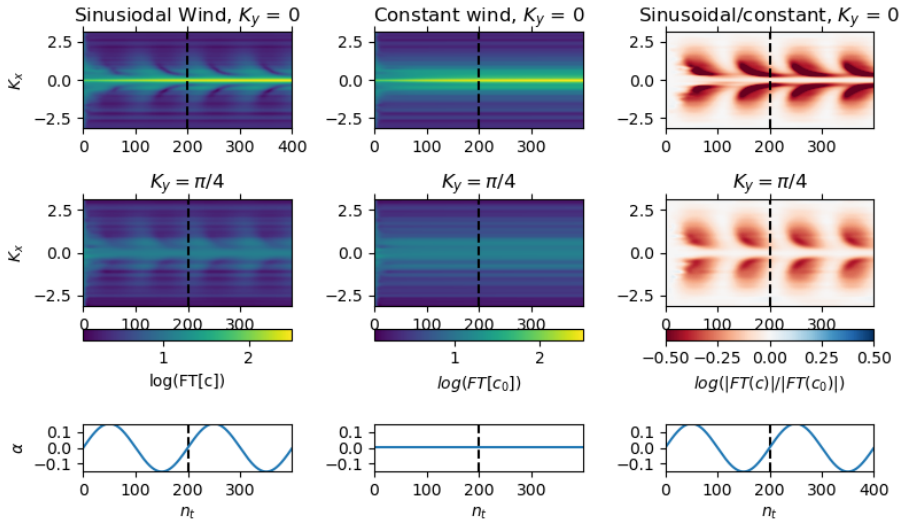

Figure 9: Plots are analogous to those of Fig.8, but with α_0 set to 0 and constant wind case is omitted since it is already represented in 8. Although with evident differences, the creation and evolution of the minima lobes in the $|FT[c]|/|FT[c_0]|$ resambles the one described above for $\alpha_0 = 0.15$. A remarkable difference with previouses plots lies in the fact that the periodicity is halved since the ratio $|FT[c]|/|FT[c_0]|$ does not depend the sign of α.

In Fig.10 analogous graphs are shown for intermediate values of α_0 to the two already presented in order to underline the effect that α_0 has on the second half of each period. Minima formed for each period are fewer but more pronounced for lower α_0.

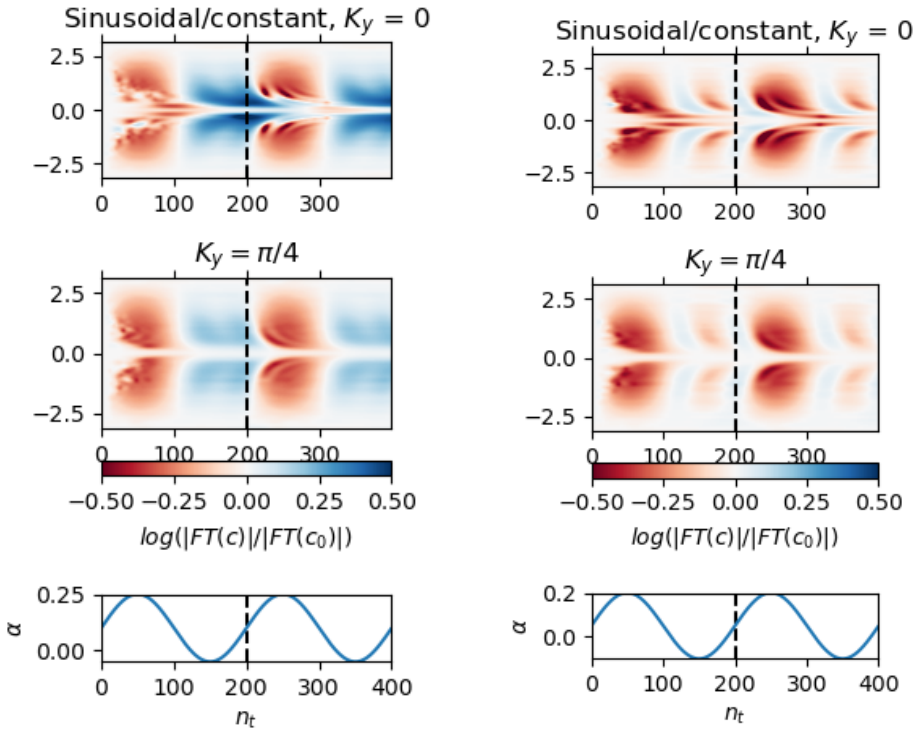

(a) $\alpha_0 = 0.10$ (b) $\alpha_0 = 0.005$

Figure 10: Plots are analogous to previouses in order to show the transition between Fig.8 and 9, varying α_0. Colorbars are the same in order to make the plots confrontable. Here is evident the effect of α_0 on the second half of the period, that now start to resemble the first half.

Another interesting comparison can be done by varying δ_α while keeping the other parameters set to the values they had in the first case presented here ($\alpha_0 = 0.15$, $\omega = \frac{2\pi}{200}$).

The most evident effect is the flattening of the differences when decreasing wind oscillations, as expected (Fig.11). As a less obvious effect, fewer minima are created and their trajectory in the k_x, t plane assumes a more horizontally elongated shape, meaning they migrate slower towards $k_x = 0$.

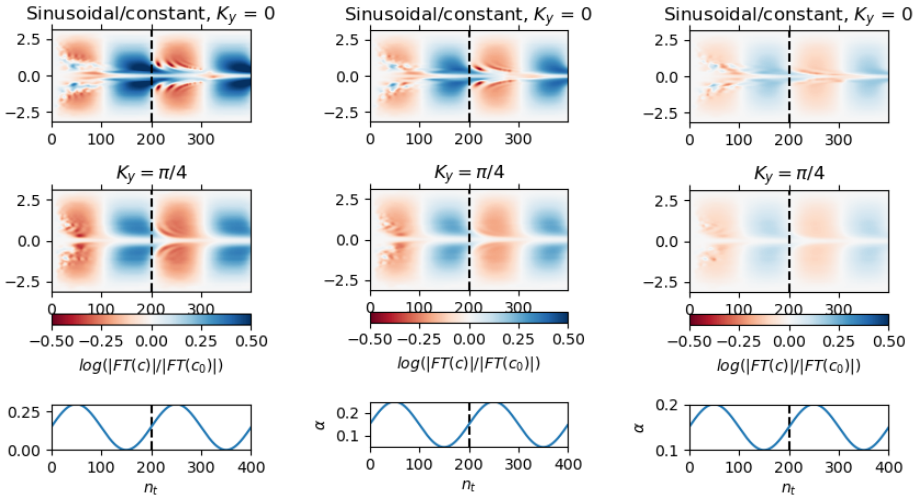

(a) $\delta_\alpha = 0.15$ (b) $\delta_\alpha = 0.01$ (c) $\delta_\alpha = 0.005$

Figure 11: Plots are analogous to previouses, now varying δ_α. Colorbars are the same in order to make the plots confrontable. As expected, maps are flattened when decreasing wind oscillations, indicating that the difference due to the wind variability are less marked. Note also that red stripes are fewer and more horizontally elongated, meaning that they move slowly towards $k_x = 0$.

Other comparisons have been made by changing the starting phase of the sine in Eq.6 and the sign of α but, as expected, no remarkable differences have been found for the stationary behaviour.

Finally we show in Fig.12 how the same plots change with ω, keeping $\alpha_0 = 0.15$ and $\delta_\alpha = 0.15$. A general trend is observable: when increasing the duration of the period more minima are created but these are less intense.[4]

[4]Interestingly, these effects observed are similiar to those obtained changing α_0. However, they are not exactly the same: for example, it is evident how the second half of the period is not significantly affected by ω, as opposed to what happens in the latter case, as discussed above in Fig.10.

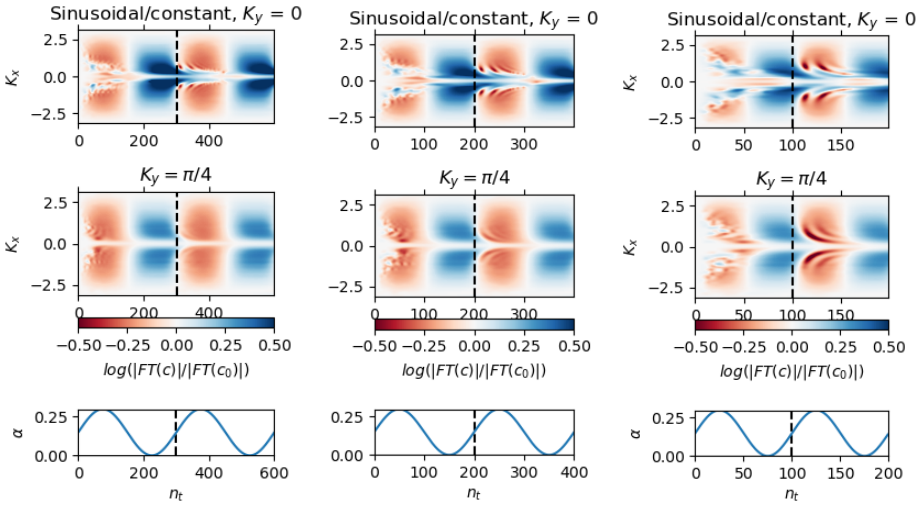

(a) $\omega = \frac{2\pi}{300}$ (b) $\omega = \frac{2\pi}{200}$ (c) $\omega = \frac{2\pi}{100}$

Figure 12: For higher ω (increasing from left to right), we observe the creation of fewer but more intense relative minima, as is particularly evident in the central row for $k_y = \pi/4$.

4 Conclusions

Sinusoidal wind affects greatly the dynamics of the typical ADR system presented here with the formation of a wiggly profile around the central peak of $|FT[c]|$ that evolves in time with the peculiar pattern described above. The main features of this behaviour persist when changing wind parameters but with some noteworthy differences. Due to the non-linearity of the system, further studies are needed in order to fully understand its dynamics. Nonetheless, we have highlighted some general trends that can be summarised as:

- To higher α_0 corresponds an increasing number of ripples, but their intensity is lowered. Furthermore, the changing of α_0 has repercussions also on the second half of the period, up to the point where for $\alpha_0 = 0$ the periodicity of $|FT[c]|$ is halved and the same features of the first half are retrieved (Fig.9).
- Lowering δ_α, as could be expected, smooths out the differences between variable and constant wind (Fig.11). It is interesting to note that δ_α influnces also the number of visible ripples and how fast they move towards $k_x = 0$ (Fig.11).
- Changing the frequency of the wind oscillations has some noteworthy consequences, somehow similiar to those of α_0: the number of minima created is higher for longer periods, although these are less marked. No significative difference is found however for the secondo half of the period (Fig.12).

We conclude by suggesting some possibles developments to the present work:

- By eliminating the periodic boundary conditions, it would be interesting to see the dependence on the wind parameters of the population flux, compared to the same system subjected to constant wind. The same study could be done for the average population (as briefly mentioned in footnote 1).
- We have followed the development of relative minima of the $|FT[c]|$ mainly by studying how their intensity depend on the wind parameters and how many are created during one period. A more quantitative study on their shape, number and relative distance as a function of said parameters could be illuminating in order to better understand the causes of these features.